Disorder-Induced Transition to Entangled Vortex Solid in Nd-Ce-Cu-O Crystal

D. Giller, A. Shaulov, R. Prozorov, Y. Abulafia, Y. Wolfus, L. Burlachkov, and Y. Yeshurun
Center for Superconductivity, Department of Physics, Bar-Ilan University, Ramat Gan 52900, Israel

E. Zeldov
Department of Condensed Matter Physics, The Weizmann Institute of Science, Rehovot 76100, Israel

V. M. Vinokur
Argonne National Laboratory, Argonne, Illinois 60439

J. L. Peng and R. L. Greene
Department of Physics and Center for Superconductivity Research, University of Maryland, College Park, Maryland 20742
(Received 26 March 1997)

Local magnetic measurements in a highly anisotropic Nd-Ce-Cu-O crystal reveal a sharp onset of an anomalous magnetization peak at a *temperature-dependent* field B_{on}. The same field marks a change in the field profiles across the sample, from profiles dominated by geometrical barriers below B_{on} to Bean-like profiles above it. The temperature dependence of B_{on} and the flux distribution above and below B_{on} imply a disorder-induced transition at B_{on} from a relatively ordered vortex lattice to a highly disordered, entangled vortex solid. Local magnetic relaxation measurements above B_{on} show evidence for plastic vortex creep associated with the motion of dislocations in the entangled vortex structure. [S0031-9007(97)04113-6]

PACS numbers: 74.60.Ge, 74.72.Jt

The nature of the different vortex phases in the mixed state of high temperature superconductors (HTS) is a topic of extensive experimental and theoretical research [1–5]. Much of the experimental work has been focused on the highly anisotropic $Bi_2Sr_2CaCu_2O_8$ (BSCCO) crystals, revealing a rich phase diagram [2,4,5]. In particular, recent local magnetization measurements [2] in BSCCO crystals revealed a sharp onset of an anomalous second magnetization peak at a field B_{on} which was interpreted as indicating a transition between two solid phases of the vortex structure [6]. An evidence for two distinct solid vortex phases in BSCCO was previously obtained in neutron diffraction [4] and μSR [5] experiments. Following these observations, a theoretical model was developed [7–9], describing a mechanism for a disorder-induced transition, from a relatively ordered vortex lattice, to a highly disordered entangled vortex solid.

The essence of this new model is that the vortex phase diagram is determined by the interplay between three energy scales: the vortex elastic energy E_{el}, the energy of thermal fluctuations E_{th}, and the pinning energy E_{pin}. The competition between the first two determines the melting line [2,10] while the competition between the last two determines the irreversibility line. Most relevant to the present work is the competition between the elastic energy and the pinning energy: At low fields the elastic interactions govern the structure of the vortex solid, forming a quasiordered lattice [11]. Above B_{on}, however, disorder dominates and vortex interactions with pinning centers result in an entangled solid where cells of the vortex lattice are twisted and dislocations proliferate [7–9,11].

The above model describes B_{on} as the intersection line of $E_{el}(B,T)$ and $E_{pin}(B,T)$ surfaces, provided that E_{th} can be neglected—a condition that is difficult to realize in most HTS systems. In this Letter, we present a study of B_{on} in a system where E_{th} can be neglected over a wide temperature range, and for the first time the details of the *temperature dependence* of B_{on} can be compared with the model predictions up to the close vicinity of T_c. This is in contrast with the BSCCO system in which E_{th} plays an important role and B_{on} is observed over a limited temperature range where it is essentially constant. In addition, we present field profiles and magnetic relaxation data below and above B_{on}. The temperature dependence of B_{on}, the field profiles, and the relaxation data imply a disorder-induced transition at B_{on} from a relatively ordered vortex lattice to a highly disordered, entangled vortex solid.

The system investigated is a $Nd_{1.85}Ce_{0.15}CuO_{4-\delta}$ (NCCO) crystal, a layered HTS with a large anisotropy (ε between $1/30$ and $1/100$) [12], however, with a relatively low transition temperature ($T_c \sim 23$ K). In this system, because of the relatively low T_c, the role of thermal energy is less significant, and one is able to examine the competition between the elastic and pinning energy over an extended temperature range.

An array of 11 Hall probes (sensitivity better than 0.1 G), based on GaAs/AlGaAs 2DEG, was in direct contact with the surface of the NCCO crystal ($1.2 \times 0.35 \times 0.02$ mm^3). The active area of each probe was 10×10 μm^2. The probes detect the component of the induction field normal to the surface of the crystal.

 0031-9007/97/79(13)/2542(4)$10.00

The inset to Fig. 1 displays typical hysteresis loops at 16 K for several probes located across the width of the sample, at distances 13, 33, 53, and 73 μm from its center. The loops are wider for probes located towards the sample center, as expected [13]. Similar to BSCCO [2], the onset of the second magnetization peak for NCCO (marked by an arrow in the figure) is sharp and occurs at the same induction field ($B_{\rm on} = 180$ G), for all the probes. The squares in Fig. 1 describe the temperature dependence of $B_{\rm on}$. Note that $B_{\rm on}$ is a continuous function of temperature all the way up to $\sim$1.5 K below T_c, where the anomaly is difficult to resolve. Also shown in Fig. 1 is the irreversibility field $B_{\rm irr}$ (circles), measured as the field above which the ascending and descending branches of the hysteresis loop coincide. There is no indication in our data for a "jump" of the magnetization in the reversible state, a jump which would indicate a first order melting transition [2].

In the context of the new model mentioned above, in the region where the thermal energy may be neglected, $B_{\rm on}$ is determined by equating the elastic energy $E_{\rm el} = \varepsilon\epsilon_0 c_L^2 a_0$ with the pinning energy $E_{\rm pin} = U_{\rm dp}(L_0/L_c)^{1/5}$ [7,8]. In these expressions, ε is the anisotropy parameter, $\epsilon_0 = (\Phi_0/4\pi\lambda)^2$ the vortex line tension, $c_L = 0.1$–0.3 the Lindemann number, $a_0 = (\Phi_0/B)^{1/2}$ the intervortex spacing, $U_{\rm dp} = (\gamma\varepsilon^2\epsilon_0\xi^4)^{1/3}$ the single vortex depinning energy, $L_0 \simeq 2\epsilon a_0$ a characteristic size of the longitudinal fluctuations, $L_c = (\varepsilon^4\epsilon_0^2\xi^2/\gamma)^{1/3} = \varepsilon\xi(j_0/j_c)^{1/2}$ the size of a coherently pinned segment of the vortex, γ the disorder parameter, $j_0 = 4\Phi_0/[3\sqrt{3}\xi(4\pi\lambda)^2]$ the depairing current, j_c the critical current of the pinning disorder, and ξ and λ are, respectively, the coherence length and the penetration depth. The equation $E_{\rm el} = E_{\rm pin}$ yields [14]

$$B_{\rm on} \approx B_0[U_0/U_{\rm dp}]^3, \qquad (1)$$

where $B_0 = c_L^2\Phi_0/\xi^2$ and $U_0 = c_L\varepsilon\epsilon_0\xi/2^{11/6}$. Note that Eq. (1) is valid only if $s < L_c < L_0$, where s is the interlayer spacing. This condition is fulfilled in NCCO where $s \approx 6$ Å, as may be verified by substituting $\varepsilon = 1/30$ [12], $\xi = 80$ Å, $\lambda = 1000$ Å [15], and $j_c \approx 10^6$ A/cm^2 [16] in the above expressions for L_c and L_0, yielding $L_c \sim 30$ Å and $L_0 \sim 300$ Å. The temperature dependence of $B_{\rm on}$ has its origin in the temperature dependence of ξ, λ, and γ. While the temperature dependence of the first two parameters is universal, that of γ is model dependent. For δT_c pinning [1], in which local suppression of T_c is the origin of pinning, $\gamma \propto 1/\lambda^4$, and Eq. (1) yields

$$B_{\rm on}(T) \propto \xi^{-3} = B_{\rm on}(0)[1 - (T/T_c)^4]^{3/2}. \qquad (2)$$

The case of δl pinning [1], where fluctuations in the electron mean free path l serve as pinning centers, is ruled out because it leads to $B_{\rm on}(T) \propto \xi$, i.e., $B_{\rm on}$ *increases* with temperature, in contrast with our experimental data.

The solid line in Fig. 1 presents a fit of the experimental data to Eq. (2), yielding $B_{\rm on}(0) = 270$ G and $T_c = 23$ K. The agreement between the calculated and measured data is apparent. Returning now to Eq. (1) we find $T_{\rm dp} = U_{\rm dp}(0) \sim 60$ K $> T_c$, confirming that thermal depinning is insignificant in our experiment.

The above analysis allows comparison of the three energy scales, $E_{\rm el}$, $E_{\rm pin}$, and $E_{\rm th}$, in our NCCO system. These energies are shown in Fig. 2(a) as a function of temperature and field. The figure demonstrates that both $E_{\rm el}$ and $E_{\rm pin}$ are decreasing functions of temperature and field, but the decrease of the elastic energy is faster, causing $E_{\rm el}(B,T)$ and $E_{\rm pin}(B,T)$ surfaces to cross each other. The projection of this crossing line on the *B-T*

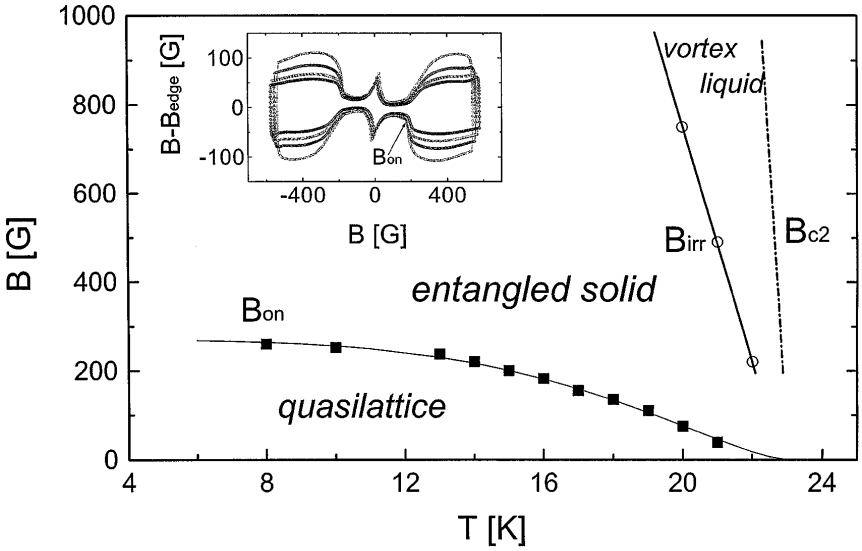

FIG. 1. Temperature dependence of the onset of the second peak $B_{\rm on}$ (squares) and the irreversible field $B_{\rm irr}$ (circles). The solid line is a fit of the experimental data to Eq. (2). The dotted line illustrates the upper critical field B_{c2}. Inset: Local magnetization vs the induction B in NCCO at $T = 16$ K, for Hall probes across the width of the sample at distances 13, 33, 53, and 73 μm from its center. The loops are wider for probes located towards the sample center. The onset of the magnetization peak at $B_{\rm on} = 180$ G is marked by an arrow.

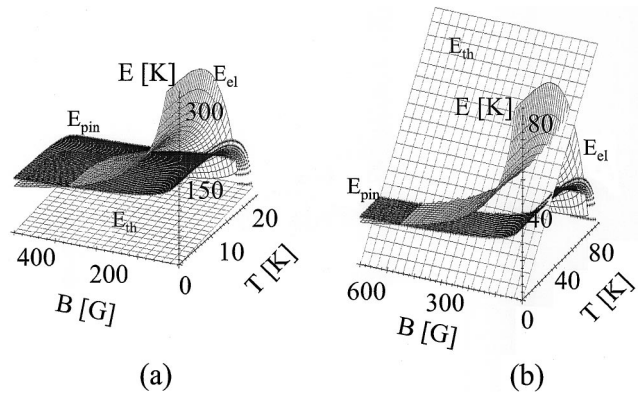

FIG. 2. Elastic ($E_{\rm el}$), pinning ($E_{\rm pin}$), and thermal ($E_{\rm th}$) energies as a function of temperature and field (a) for NCCO and (b) for BSCCO. $E_{\rm th}$ is negligible in most of the temperature range in NCCO but only at low temperatures in BSCCO. In these temperature ranges, $B_{\rm on}(T)$ is the projection of the crossing line $E_{\rm el} = E_{\rm pin}$ on the B-T plane. In BSCCO, the melting line is the projection of the crossing line $E_{\rm el} = E_{\rm th}$ on the B-T plane.

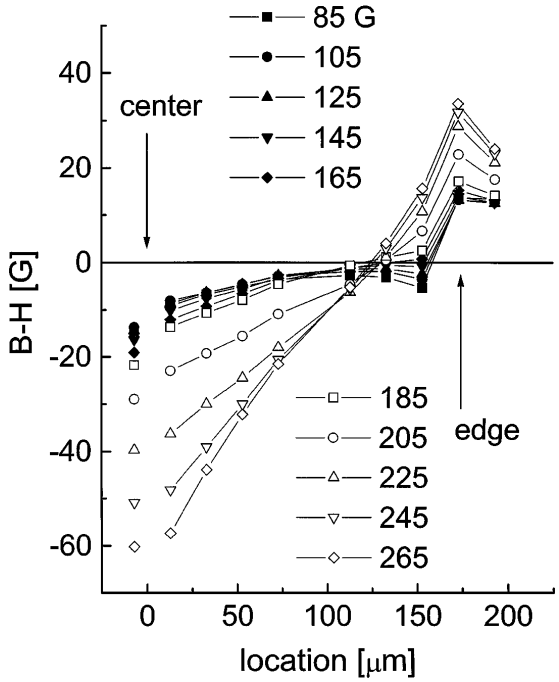

FIG. 3. Typical induction profiles at 16 K across the NCCO sample. For fields below $B_{\rm on} \approx 180$ G the profiles exhibit a maximum (around 120 μm), typical of surface and geometrical barriers in the presence of weak bulk pinning. For fields above $B_{\rm on}$, the profiles are Bean-like with much larger gradients, indicating the onset of strong pinning.

plane is the $B_{\rm on}(T)$ line. Note that the thermal energy is well below $E_{\rm el}$ and $E_{\rm pin}$ for most of the temperature range. For comparison, we show in Fig. 2(b) the same plot for BSCCO using the parameters $T_c = 90$ K, $\varepsilon = 1/100$, and $B_{\rm on}(0) = 450$ G. As apparent from the figure, in BSCCO $E_{\rm th}$ plays an important role, and one can identify both $B_{\rm on}(T)$ and the melting line $B_m(T)$. Note that the crossing line of $E_{\rm el}$ and $E_{\rm pin}$ can be viewed as $B_{\rm on}(T)$ only at low temperatures where the contribution of $E_{\rm th}$ can be neglected. Figure 2(b) indicates that in this region $B_{\rm on}(T)$ is temperature independent.

Our experimental data for the field profiles above and below $B_{\rm on}$ are consistent with the disorder-induced phase transition scenario. Figure 3 shows typical profiles measured at 16 K. For fields below $B_{\rm on}$ the profiles have a shape characteristic of geometrical barriers with weak bulk pinning [17], exhibiting maxima around 120 μm from the center. For fields above $B_{\rm on}$, the profiles are Bean-like with much larger gradients, indicating the onset of strong pinning. The figure demonstrates that a small change ($\leq$20 G) around 200 G causes the transition between the two types of profiles.

The proliferation of dislocations in the vortex structure of the entangled phase should affect the mechanism of the flux creep in the system. Specifically, we expect that dislocation mediated plastic creep will prevail at high enough fields. One of the main characteristics of such a flux creep mechanism is the decrease of U with the increase of the induction field B [18]. This is to be contrasted with the collective (elastic) creep mechanism for which U increases with B [1]. From our local magnetic relaxation data, utilizing the technique described in Ref. [19], we determine U as a function of j for various fields. Typical results are shown in Fig. 4 for $T = 13$ K. The figure demonstrates a clear crossover in the slope of $U(j)$ around $B \approx 900$ G. The parameter $\mu \equiv -\partial \ln U/\partial \ln j$ attains values 0.8–1.1 below 900 G, consistent with the predictions of the collective (elastic) creep model. However, above this field μ decreases to low values ($\simeq$0.2) which cannot be explained in the framework of the collective creep model for this field range. Figure 4 further shows a nonmonotonous dependence of U on B; U increases with B for fields below 900 G and decreases with B above this field, as indicated by the right and left vertical arrows in Fig. 4, respectively. While the increase of U with B is consistent with elastic creep, the decrease of U with B shows an evidence for plastic vortex creep associated with the motion of dislocations in the vortex lattice [20]. It should be noted that although dislocations start to form immediately above $B_{\rm on} \approx 200$ G, plastic creep cannot dominate the dynamics until the activation energy $U^{\rm pl}$ for plastic creep drops below the activation energy $U^{\rm el}$, for the collective (elastic) creep. In the case shown in Fig. 4, this crossover occurs around $B = 900$ G.

In conclusion, in the NCCO system, because of its relatively low T_c, one can focus on the competition between $E_{\rm pin}$ and $E_{\rm el}$ over an extended range of temperature, ignoring the contribution of $E_{\rm th}$. In contrast to BSCCO crystals in which $B_{\rm on}$ is observed over a limited temperature range where it is essentially constant, in the NCCO system $B_{\rm on}$ exhibits strong temperature dependence up to the close vicinity of T_c. This temperature dependence excludes interpretation of the second peak based

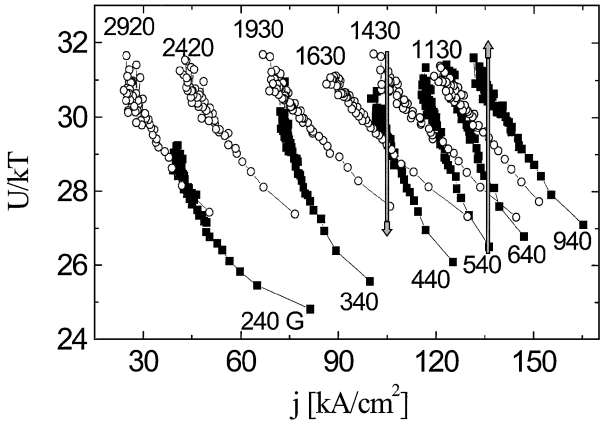

FIG. 4. Activation energy for flux creep U as a function of current density j at $T = 13$ K, for various fields. The squares and the circles refer to fields below and above the peak, respectively. A crossover in the slope of $U(j)$ near $B = 900$ G is evident. The right arrow indicates the increase of U as B increases from 540 to 640 and 940 G. The left arrow indicates the decrease of U as B increases from 1430 to 1630 and 1930 G.

on a dimensional crossover in the vortex structure [21] or matching effects [6], as both imply temperature *independence* of B_{on}. On the other hand, our analysis shows that the temperature dependence of B_{on} is consistent with the new model which ascribes the onset of the second magnetization peak to a disorder-induced transition in the vortex solid. This scenario is consistent with the observation of a crossover in the field profiles across the sample, from profiles characteristic of geometrical barrier with weak pinning at fields below the onset, to Bean-like profiles at fields above the onset. A consistent picture also emerges from our local magnetic relaxation measurements above B_{on} which show evidence for plastic vortex creep associated with the motion of the dislocations in the vortex structure.

This work was supported in part by The Israel Science Foundation and by the Heinrich Hertz Minerva Center for High Temperature Superconductivity. Y. Y. and E. Z. acknowledge support from the U.S.-Israel Binational Science Foundation. V. M. V. acknowledges support from Argonne National Laboratory through the U.S. Department of Energy, BES-Material Sciences, under Contract No. W-31-109-ENG-38. R. L. G. acknowledges support from the NSF, Contract No. DMR-9510475.

[1] G. Blatter *et al.*, Rev. Mod. Phys. **66**, 1125 (1994).
[2] B. Khaykovich *et al.*, Phys. Rev. Lett. **76**, 2555 (1996).
[3] A. Schilling *et al.*, Nature (London) **382**, 791 (1996).
[4] R. Cubitt *et al.*, Nature (London) **365**, 407 (1993).
[5] S. L. Lee *et al.*, Phys. Rev. Lett. **71**, 3862 (1993).
[6] The second magnetization peak observed in other HTS systems, e.g., in Y-Ba-Cu-O (YBCO), does not exhibit a sharp onset as in BSCCO, and it may be of a different origin. The various models proposed include inhomogeneities of the sample [M. Daeumling *et al.*, Nature (London) **346**, 332 (1990); L. Klein *et al.*, Phys. Rev. B **49**, 4403 (1994)], matching effects [R. Yoshizaki *et al.*, Physica (Amsterdam) **225C**, 299 (1994)], and dynamic effects [L. Krusin-Elbaum *et al.*, Phys. Rev. Lett. **69**, 2280 (1992)].
[7] D. Ertas and D. R. Nelson, Physica (Amsterdam) **272C**, 79 (1996).
[8] V. Vinokur, B. Khaykovich, E. Zeldov, M. Konczykowski, R. A. Doyle, and P. Kes (unpublished).
[9] T. Giamarchi and P. Le Doussal, Phys. Rev. B **55**, 6577 (1997); Y. Y. Goldschmidt, Phys. Rev. B (to be published); J. Kierfeld, Report No. cond-mat/9609045.
[10] H. Safar *et al.*, Phys. Rev. Lett. **70**, 3800 (1993).
[11] T. Giamarchi and P. Le Doussal, Phys. Rev. Lett. **72**, 1530 (1994); J. Kierfeld, T. Nattermann, and T. Hwa, Phys. Rev. B **55**, 626 (1997); D. S. Fisher, Phys. Rev. Lett. **78**, 1964 (1997).
[12] T. W. Clinton *et al.*, Physica (Amsterdam) **235-240C**, 1375 (1994).
[13] R. Prozorov *et al.*, J. Appl. Phys. **76**, 7621 (1994).
[14] The calculations of Ref. [7] yield a similar expression with an exponent of $10/3$ instead of 3. This leads to an insignificant difference in the final result for B_{on} [Eq. (2)] where the exponent becomes $14/9$ instead of $3/2$.
[15] The penetration depth λ was estimated from our magnetic measurements of the lower critical field and is consistent with C. Yeh *et al.*, Phys. Rev. B **48**, 9861 (1993).
[16] A. I. Ponomarev *et al.*, JETP Lett. **62**, 517 (1995); Dong Ho Wu *et al.*, Phys. Rev. Lett. **70**, 85 (1993).
[17] E. Zeldov *et al.*, Phys. Rev. Lett. **73**, 1428 (1994).
[18] V. B. Geshkenbein *et al.*, Physica (Amsterdam) **162-164C**, 239 (1989).
[19] Y. Abulafia *et al.*, Phys. Rev. Lett. **75**, 2404 (1995); J. Appl. Phys. **81**, 4944 (1997).
[20] Y. Abulafia *et al.*, Phys. Rev. Lett. **77**, 1596 (1996). It is interesting to note that our results in NCCO resemble those obtained in YBCO, despite the qualitative differences in the shape and in the field range of the fishtails in these systems.
[21] T. Tamegai *et al.*, Physica (Amsterdam) **213C**, 33 (1993); S. Ooi *et al.*, J. Low Temp. Phys. **105**, 1011 (1996).